SUPERIOR COATING TECHNOLOGY FOR ADVANCED COLD WIRE DRAWING OF SPRING STEELS

MIROSLAV PISKA, TEREZA HAVLIKOVA AND ZUZANA VNUKOVA

Brno University of Technology, Faculty of Mechanical Engineering, Department of Manufacturing Technology, Brno, Czech Republic

DOI: 10.17973/MMSJ.2022_11_2022132

e-mail : piska@fme.vutbr.cz

ABSTRACT

The technology of cold wire drawing belongs to an ancient class of technologies, but their use lasts for centuries. Today, special forming machines, advanced tool materials and effective lubricants are used. In this paper, a progressive physical vapour technology (PVD) of coating for inner surfaces is used which resulted in significant prolongation of tool life. The technology of HiPIMS (High-power Impulse Magnetron Sputtering) exhibited excellent performance in protective (Al,Ti)N coating of whole inner surfaces that are in contact with the drawn wire which is impossible to do with other coating techniques. The increase in production of the drawn steel spring wire by the coated die by more than 100% was excellent, and it opens new horizons to some similar technological applications.

KEYWORDS

HiPIMS, PVD, coating, drawing die, cold wire drawing, cold forming, wear

1 INTRODUCTION

The main goal of a wire drawing operation is to reduce the cross-sectional area of a wire to adjust it to a certain diameter. To accomplish this, the wire is drawn through a conical converging die or multiple arrangements of the tools.

Cemented tungsten carbides are widely used for this application due to their high hardness, acceptable toughness and very good wear resistance at relatively low costs. However, these days the tungsten carbide dies face challenges to satisfy the modern industry demands as they seem to be insufficient in meeting all the requirements for a tool lifetime and high quality of drawing. The problem is highlighted in spring steels that undergo heat treatment and dynamic loading afterwards.

During the forming process, high compressive and shear stresses act on the surface of the die which initiate the wear of the tool. Wear is one of the main reasons for tool failure in mass production, according to [Panjan 2005], it is the main cause of die replacement in 70 % of cases after use. [Pirso 2004] found that the wear of cemented carbides is caused mainly by the removal of the cobalt binder followed by fracture of intergranular boundaries and fragmentation of carbide grains. The loosening of the grains then leads to the abrasive wear of the die. Another typical wear mechanism in wire drawing is adhesion. The probability of adhesion grows with the value of normal stress, chemical affinity and sliding distance of two materials in contact.

The wear of a die has a direct impact not only on the lifetime and costs of the tool but also on the quality of the drawn wire which can be damaged due to the degradation of the die surface. The tool life can be prolonged by cooling and lubricating the tool and wire with soaps, oils, polymers etc. [Piska 2022].

Anyway, hard coatings have been successfully used to improve the performance of tungsten carbide drawing dies and minimize their wear by increasing their hardness, wear resistance and chemical inertness. The main drawbacks of the coating technologies can be seen in high temperatures for Chemical Vapour Technologies (CVD), affecting the precision and surface quality, or directional distribution of hard particles preventing a deeper penetration in the conical and cylindrical cavity of dies at Physical Vapour Technologies (PVD). Conventional PVD techniques like arc evaporation or magnetron sputtering are line-of-sight processes which means that the coating-forming material is transported in a straight path from the source to the substrate and is predominantly deposited on the flat front sides of the substrate. This phenomenon called the shadowing effect results in a growth of an inhomogeneous film on the sidewalls of interior surfaces with many growth defects (columnar structure, nodular defects, pores, etc.) [Panjan 2020]. These growth defects degrade the functionality of the coating as they are also the starting points for environmental attacks like corrosion [Korhonen 1994] or oxidation [Braak 2018].

To suppress this problem a higher ionization rate of deposition material can be used. The incoming particles have higher arrival energy and can align themselves in the shape of the substrate. This is typical for ionized PVD techniques like High-power Impulse Magnetron Sputtering (HiPIMS), firstly reported by [Kouznetsov 1999] and developed by many research groups since then.

The principle of the HiPIMS deposition method is the same as for conventional magnetron sputtering. It is a plasma-based technique where atoms of inert gas (commonly Ar or Kr) are ionized and accelerated towards the negatively biased target (cathode). The interaction between the charged particles and the target surface causes an ejection of atoms of the target material which then condensate on the substrate and create a thin film [Mattox 2010]. The main thing that changes is the power source.

The power applied to the cathode in conventional continuous DC magnetron sputtering is limited by the overheating of the target. The resulting plasma density in the close vicinity of the target is in the order of 10^{17} m^{-3} [Bradley 2001]. In this low-density plasma, the degree of ionization of sputtered material is only a few per cent [Christou 2000]. To increase the plasma density, the power is applied in pulses (50–200 μs) of high power (cathode voltage 500–2 000 V, current densities of up to 3–4 $A.cm^{-2}$, peak power densities in the range of 0.5–10 $kW.cm^{-2}$) with a low duty cycle (on/off ratio 0.5–5 %) [Gudmundsson 2012].

By the HiPIMS discharge, a plasma density of up to 10^{19} m^{-3} can be achieved which results in the ionization degree of the target material up to 90 % [Bohlmark 2005]. The presence of energetic particles in the flux of coating material not only enables the coating of substrates placed perpendicularly to the target [Alami 2005] but also effectively changes the morphology and associated properties of the coating. The coatings deposited by HiPIMS were reported to have smooth droplet-free surface [Sarakinos 2007], increased hardness [Engwall 2019], density [Samuelsson 2010] and adhesion [Ehiasarian 2007]. In addition to that, HiPIMS also allows better control of the thin film growth

by phase tailoring [Alami 2007], selective substrate biasing [Greczynski 2014] or guiding of the deposition material to the desired area of the substrate [Bohlmark 2006].
Therefore the HiPIMS has been proven to be a very promising technology for the deposition of hard coatings as it combines the many advantages of conventional magnetron sputtering and arc evaporation.
Anyway, drawing is an important technological operation for the production of the cylindrical profile before the surface finishing and heat treatment of the spring steel wire follow. Therefore, surface roughness is only one of major criteria for a safe and stabilized process. The overall quality and integrity of the surface also include appearance of cracks, scratches, production of oxides and other phenomena like galling which frequently occurs for drawing with uncoated tool. Galling welds small particles of the wire material to the die first and after reaching a critical size it can be torn and squeezed into the processed wire with extreme difficulty to find this defect or disruption of the material integrity.

The objective of the present study was to evaluate the possibility of using the HiPIMS for coating wire drawing dies used for spring steel drawing and to compare the effect to an uncoated tool where undesirable phenomenon like galling can reduce significantly the quality of drawn wires.

2 EXPERIMENTAL

Three experimental dies made of tungsten carbide (59.7 at.% C, 33.9 at.% W, 6.5 at.% Co) were manufactured in a standard way and used for this study. The dimensions of the tool are shown in Fig. 1. The surfaces of the die were abrasively polished with diamond pastes (with grain sizes 5, 2, 1, and 0.25 µm) to surface roughness Ra 0.04–0.05 µm.

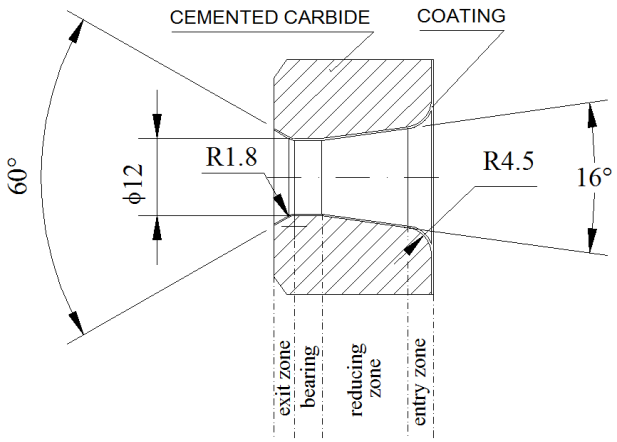

Figure 1. Dimensions of the used drawing die

The PVD coating was made by the company CemeCon s.r.o., Ivančice, Czech Republic using the coating unit CC800® HiPIMS (CemeCon, Wurselen, Germany). The coating unit has six cathodes equipped with shutters. Two cathodes with pure Ti targets (99.999%) were used in DCMS mode for etching and four Ti targets with embedded Al slugs were powered by HiPIMS to provide the coating material. The die was placed at the central substrate table and the axis of the die was oriented perpendicularly to the target surface.

Prior to the coating, etching with Ti ions was performed. The average power on the cathodes was 11.95 kW. A bias voltage of –59 V was applied to the substrate table. A mixture of nitrogen, argon and krypton gases was used, with flow rates of 240, 311 and 213 ml.min^{-1}, respectively. The deposition rate was 39 nm.min^{-1} approximately.

The protective coating synthesized on the die was FerroCon®, which is an (Al,Ti)N-based coating of anthracite colour providing the microhardness 3 800 HV0.05, and operating temperature up to 1 100 °C [CemeCon s.r.o. 2022].

To measure the real coating thickness the high-quality cross-section, made in five machining passes, through the die was made by the EDM machine AgieCharmilles CUT E 350 (GF Machining Solutions, Brno). Its average roughness Ra was below 0.1 µm and sharp corners were preserved.

The scanning electron microscope MIRA3 (TESCAN, Brno, Czech Republic) was used for analyses of the secondary and backscattered electrons (SE, BSE), energy-dispersive X-ray spectroscopy and measurement of the real thickness of the coating – Fig. 2, 3.

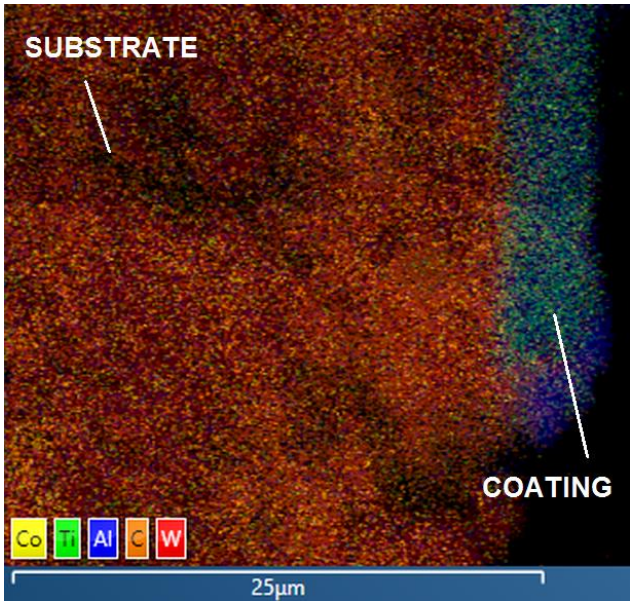

Figure 2. Distribution of selected elements at the coated and polished cross-section of the die

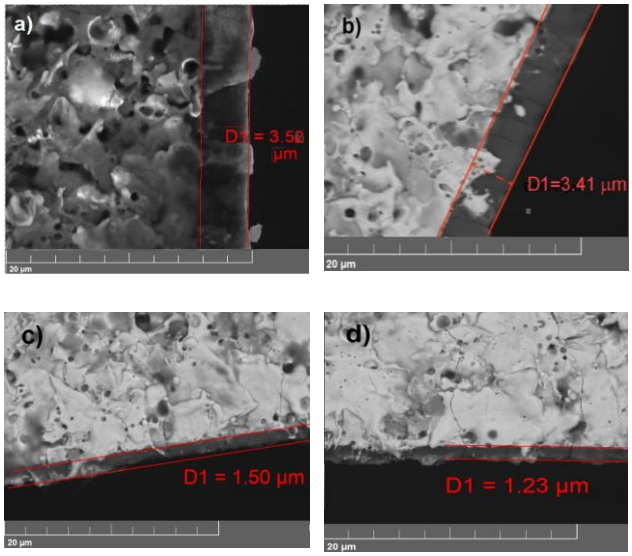

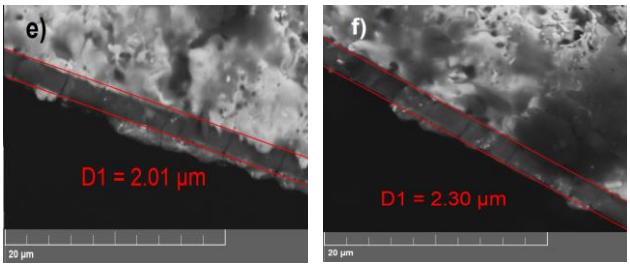

Figure 3. Thickness of the PVD layer along the die (SEM analysis)

The wear of the dies was evaluated by the scanning electron microscopy also, using a backscattered secondary electrons (BSE) detector. The Carl Zeiss Stemi 2000-C stereo zoom microscope and confocal microscope Alicona IF-G5 (Bruker Alicona, Graz, Austria) were used to observe the critical defects on the wires and measure the wire surface roughness. The surface of the wire samples was evaluated in a perpendicular direction to the drawing direction.

The overview of the thickness along the die just after deposit of the protective coating can be seen in Fig. 4. The covering of all loaded surfaces, even at the exit part of the die is astonishing and confirms a good performance of the PVD technology.

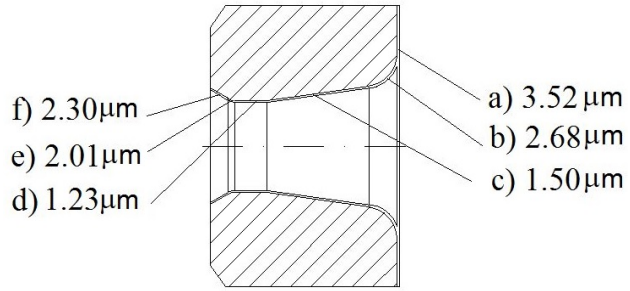

Figure 4. Overview of the coated thickness along the die after the PVD HiPIMS coating

The performance tests were made in real manufacturing conditions. A standard industrial drawing machine was used to realize these experiments – Fig. 5. The drawn material was low-alloy chromium steel in a hot-rolled state, the initial diameter of the wire was 14±0.4 mm.

The chemical composition and mechanical properties according to CSN EN 10089 can be seen in Tab. 1 and Tab. 2. The drawing speed was 0.8 $m.s^{-1}$ and solid polymer soap Traxit (a dry lubricant based on calcium $Ca(OH)_2$ and sodium soaps (NaOH), potassium hydroxide (KOH), and other ingredients, made in granular shapes) was used as the lubricant. Two dies were finally tested and compared (the uncoated one to the coated one) to quantify the effect of the coating. The criterion for the die replacement was the quality of the wire surface – an appearance of a scratch or a peak on the drawn material surface).

The quality of the drawn surface was evaluated and compared continuously using a special device for surface analysis (integrating also the principle of the eddy current method) and separately in a surface metrology laboratory (special samples were cut off from the entry and exit of the wire passing. Wire surface topography of the samples (without any chemical cleaning) was examined by scanning electron microscopy using a secondary electrons (SE) detector. The surface of the wires can be seen in Fig. 6a (for the coated die), and in Fig. 6b (for the uncoated die). The lubrication residues on the drawn surfaces have been found in both cases. The progress of wire surface roughness during the performance tests was evaluated by a non-contact measurement system InfiniteFocusG5. The measured surface of the wire samples (after 20 minutes of ultrasonic cleaning in ethyl alcohol, with the cleaner Neyson, 15 l, 40 kHz) was evaluated in the perpendicular orientation to the drawing direction.

Chemical element	Weight per cent [%]
C	0.51–0.59
Si	1.20–1.60
Mn	0.5–0.8
P	max. 0.025
S	max. 0.025
Cr	0.5–0.8
Cu + 10 Sn	< 0.6
Fe	balance

Table 1. Chemical composition (in wt.%) of the steel according to CSN EN 10089

Parameter	Value
Tensile strength	1 450–1 750 MPa
0.2% proof stress	min. 1 300 MPa
Elongation at fracture	min. 6 %
Reduction in cross-section at fracture	min. 25%
Brinell hardness	max. 280

Table 2. Mechanical properties of the steel according to CSN EN 10089

3 RESULTS AND DISCUSSION

The lifetime of the tool protected with the (Al,Ti)N coating was exactly doubled (there were drawn three coils vs six coils of the raw wire). For the coated die, around 16 500 kg of good quality steel wire was drawn while for the uncoated one it was only around 8 250 kg which corresponds to 18 704 m and 9 352 m of finished wire of 12 mm in diameter.

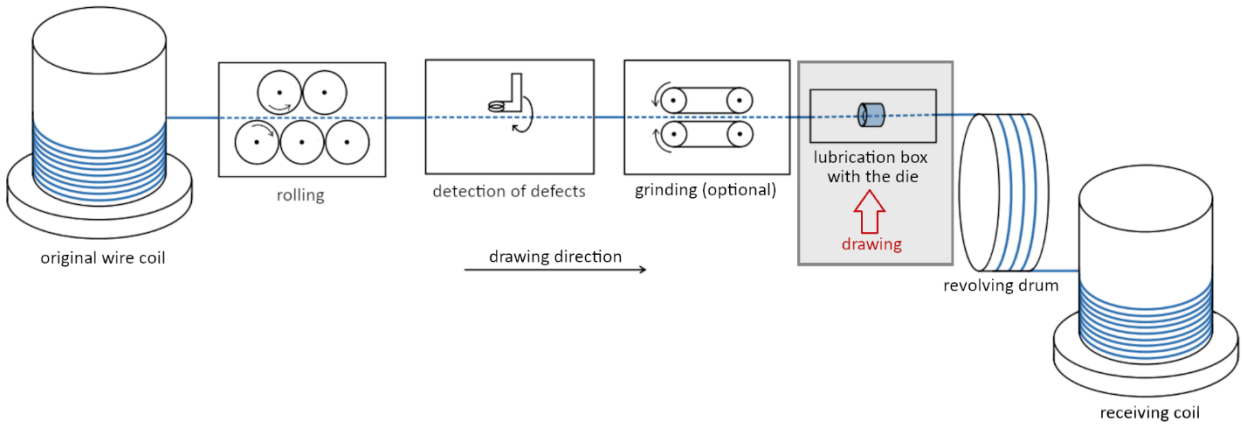

Figure 5. Schematic representation of a wire drawing machine

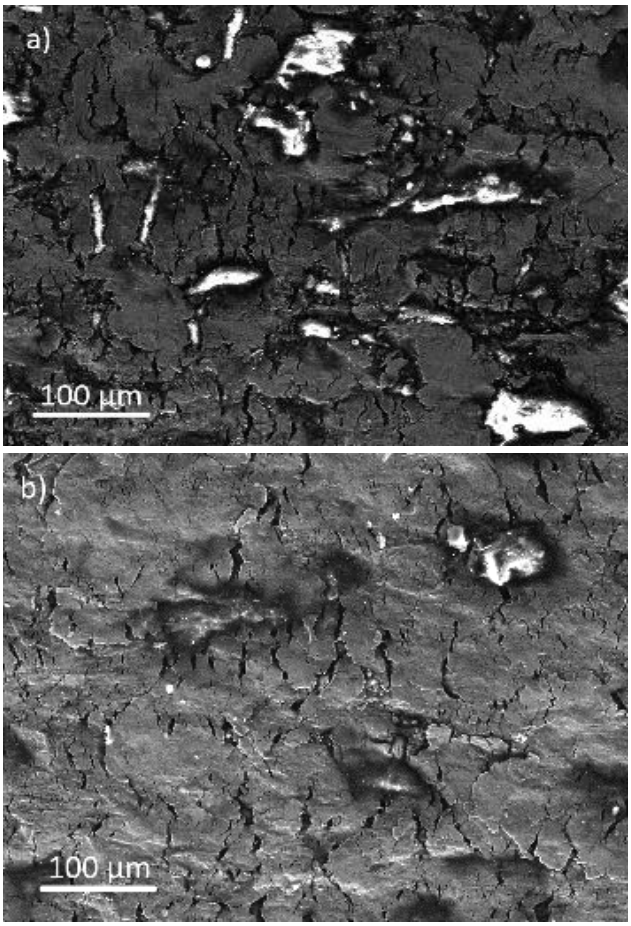

Figure 6. SEM micrographs (SE) of the wire surface after drawing with the (a) coated die, (b) uncoated die

Typical roughness profile measurement and surface topography (after the use of Gaussian filter) for the wire drawing made with the coated tool are shown in Fig. 7.

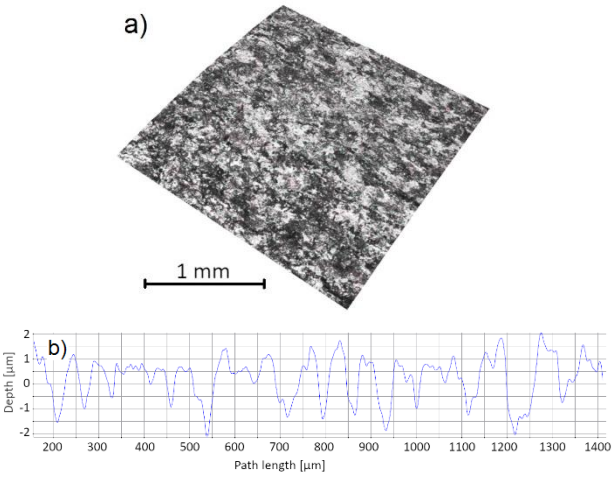

Figure 7. Typical (a) surface topography and (b) roughness profile measurement of a wire drawn with the coated tool

Measurements of Ra (arithmetic average roughness) and Rz (average maximum height) were selected as typical variables used in this technology – Fig. 8. Manufacturer's requirement to produce wires of Ra inferior to 1.6 µm was satisfied in both cases (coated and uncoated die). Ra values for the wire drawn with the coated tool were higher (Ra = 0.90±0.08 µm for the first coil, Ra = 0.95±0.07 µm for the third coil and Ra = 0.98±0.06 µm for the sixth – the last coil). This fact can be explained by a higher hardness of the coated surface which can cause an elevated roughness of drawn profiles. In this case, both Ra and Rz evolutions during the tests can be considered as slowly rising without any noticeable instabilities. As for the wire drawn by the uncoated die, Ra values are lower (Ra = 0.81±0.04 µm for the first coil, Ra = 0.85±0.05 µm for the third –the last coil). However, for the last coil drawn by the uncoated tool, a non-standard high value of Rz = 5.21±0.2 µm can be observed. This unstable behaviour can be caused by the wear of the die, which will be discussed later in this study.

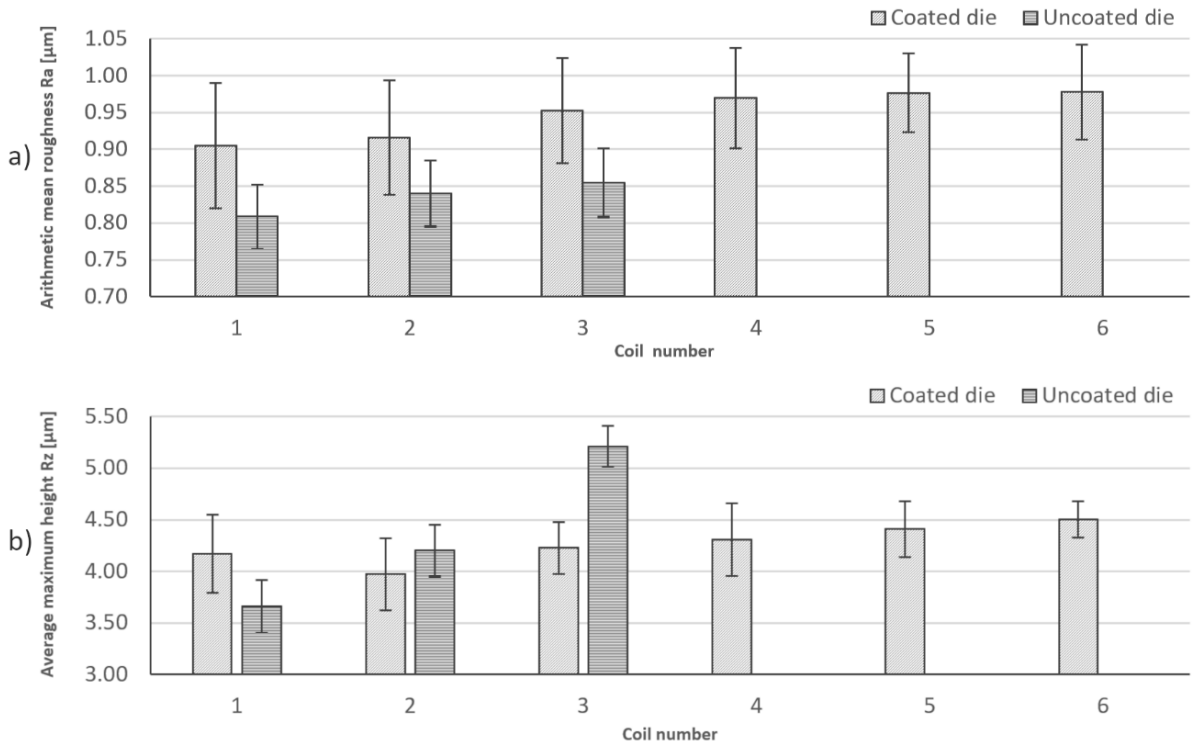

Figure 8. Evolution of wire surface roughness during the performance test – (a) Ra, (b) Rz

For the coated die a large amount of abrasive wear can be observed in the reducing zone. The "wear ring" can be seen in Fig. 9a, this is the area where the wire gets firstly in contact with the die. Very high contact pressure and shear stress acting on the die can be expected in this area. This resulted in partial removal of the coating – see Fig. 9b. Abrasive scars in the direction of the drawing were present (Fig. 9c) and a torn lump of the die material was also found – see Fig. 9d. Another zone significantly worn by abrasion is the bearing. The surface of the coated die is free from adhered workpiece material. The critical wear mechanism for the coated die was abrasion.

The tool was replaced because a scratch (Fig. 10a) about 5 µm deep (Fig. 10b) appeared across the whole length of the drawn wire.

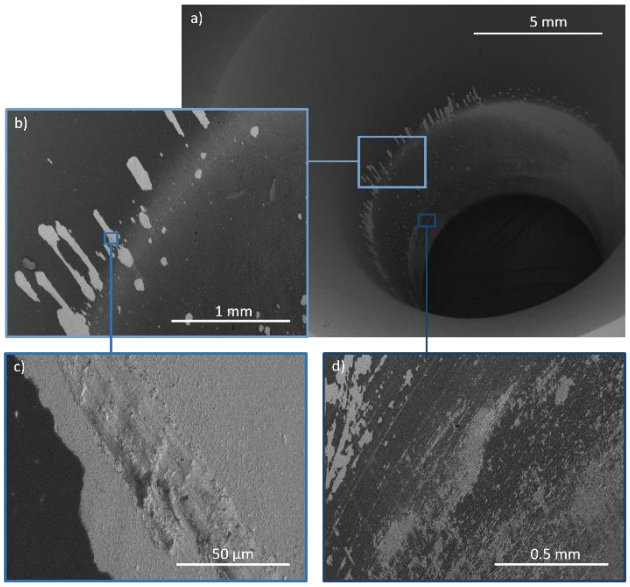

Figure 9. SEM micrographs (BSE) of the wear surface of the coated die, (a) main view with visible "wear ring", (b) removal of the coating in the reducing zone, (c) abrasive scars in the bearing, (d) torn lump of material in the reducing zone

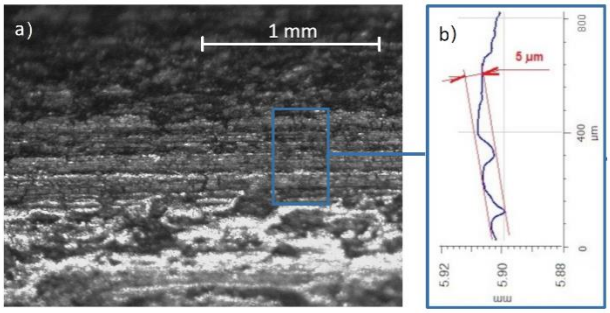

Figure 10. Micrographs of the critical defect (a) on the wire drawn by the coated die – scratch about 5 µm deep, (b) profile measurement of the depth

The wear of the uncoated tool can be seen in Fig. 11a–d. For the uncoated die there is a significant abrasion of the bearing in a form of longitudinal grooves (Fig. 11c). Compared to the coated die, the mechanism of abrasion was less dominant. The uncoated die had a higher material pick-up tendency, and a large part of the drawing cone was covered by adhered workpiece material built-up layer (Fig. 11b, Fig. 11d). This wear mechanism, also known as galling, explains the reason for the failure of the tool.

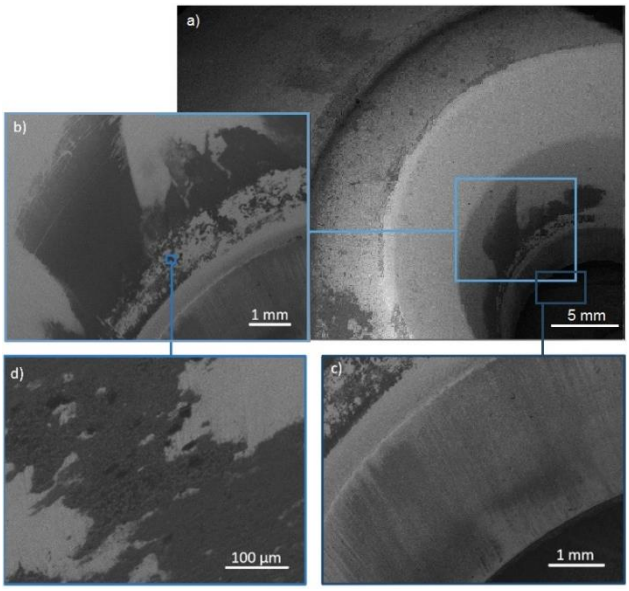

Figure 11. SEM micrographs (BSE) of the wear surface of the uncoated die, (a) an overview, (b) the wear in the reducing zone, (c) the longitudinal abrasive grooves in the bearing area (d) the adhered workpiece material in the reducing zone

Right before the failure, wire surface quality radically changed on a section corresponding to 250 mm of wire. Micrographs in Fig. 12a–e picture this evolution, the surface was examined at 5 spots, separated by 50 mm. First, a characteristic pattern of continuous lines appeared on the surface, indicating a breakthrough of the surface oxides (Fig. 12a). Transversal traces visible by naked eye can be observed in the next stage (Fig. 9b). The last three sections (Fig. 12c–e) were marked with a disruption of surface integrity due to micro-welding between the wire and the die. The change in the colour of the wire surface (from silver to brown and finally dark blue) indicates the increasing temperature caused by friction in the contact zone. Based on the observed colours, the temperature in the contact zone could go up to 250–300 °C.

The last studied parameter was the temperature of the wire after exiting the drawing die. For the first three coils (for the coated and uncoated tool), the temperature was measured at both ends of the coil. The measured values are gathered in Tab. 3. The wire was warming up more when it was drawn by the coated die. (Al,Ti)N coating has approximately ten times lower thermal conductivity (4.5–7.5 $W.m.K^{-1}$) **[Kalss 2006]** compared to the tungsten carbide **[Schultrich 1988]** so the heat is absorbed more by the wire than by the tool. This theory is confirmed by the fact that the temperature stays stable during the drawing (approximately the same value for the beginning and end of the coil). Therefore, the temperature influence on the tool is lower and the tool is more protected from undesirable changes of structural and mechanical properties, as confirm **[Pirso 2004]** and **[Panjan 2005]** also.

Coated die		Uncoated die	
Temperature [°C], beginning of coil	Temperature [°C], end of coil	Temperature [°C], beginning of coil	Temperature [°C], end of coil
100.2±1.8	99.5±1.8	90.3±2.1	93.3±2.7

Table 3. Wire temperature after exiting the drawing die

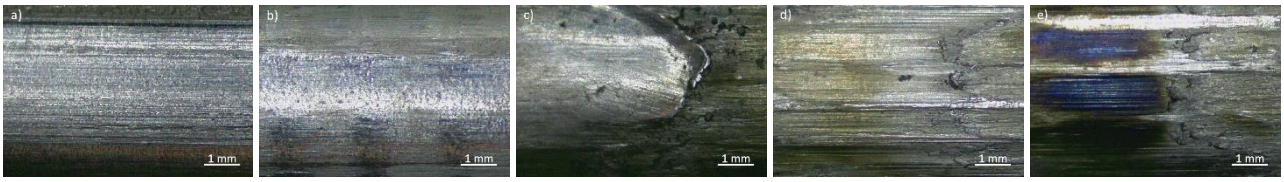

Figure 12. Micrographs of the critical defect evolution on the wire drawn by the uncoated die – (a) surface without defect, (b) visible waviness, (c, d, e) disruption of the surface integrity due to galling

4 CONCLUSIONS

The work conducted in research laboratories and industrial companies confirmed a unique advantage of the HiPIMS technology that resulted in a superior quality of the forming die coating, good integrity along the inner surface and a longer tool life. A lower coefficient of friction at the interface, the high hardness of the (Al,Ti)N coating and the lower thermal conductivity improved the plastic flow of the drawn wire with excellent forming performance. The following research will be devoted to improve and optimize the die design.

ACKNOWLEDGEMENTS

This research was funded by the Ministry of Industry and Trade, The Czech Republic. PID: grant FV40313, Application of the New Surface Treatment Technologies in Metal Packaging Industry and by the Brno University of Technology, Faculty of Mechanical Engineering, Specific research „Modern technologies for processing advanced materials used for interdisciplinary applications", FSI-S-22-7957. A special thanks belong to the company GF Machining Solutions, Brno, Czech Republic for their kind help in the technology of EDM, to the company CemeCon, s.r.o., Ivancice for HiPIMS technology and to Mr. Phillip Jones for his English corrections.

REFERENCES

[Panjan 2005] Panjan, P., Boncina, I, Bevk, J., Cekada, M. PVD hard coatings applied for the wear protection of drawing dies. Surface and Coatings Technology, 2005, Vol.200, No.1–4, pp 133–136, ISSN 02578972

[Pirso 2004] Pirso, J., Letunovits, S., Viljus, M. Friction and wear behaviour of cemented carbides. Wear, 2004, Vol.257, No. 3–4, pp 257–265, ISSN 00431648

[Piska 2022] Piska, M., Sliwkova, P., Vnukova, Z., Petrenec, M., Sedlakova, E. Exquisite Energy Savings at Cold Metal Forming of Threads through the Application of Polymers. Polymers, 2022, Vol.14, No.6, ISSN 2073–4360

[Panjan 2020] Panjan, P., Drnovsek, A., Gselman, P., Cekada, M., Panjan, M. Review of Growth Defects in Thin Films Prepared by PVD Techniques. Coatings, 2020, Vol.10, No.5, ISSN 2079-6412

[Korhonen 1994] Korhonen, A. S. Corrosion of thin hard PVD coatings. Vacuum, 1994, Vol.45, No.10–11, pp 1031–1034

[Braak 2018] Braak, R., May, U., Onuseit, L., Repphun, G., Guenther, M., Schmid, C., Durst, K. Accelerated thermal

degradation of DLC-coatings via growth defects. Surface and Coatings Technology, 2018, Vol.349, pp 272–278, ISSN 02578972

[Kouznetsov 1999] Kouznetsov, V., Macak, K., Schneider, M., Helmersson, U., Petrov, I. A novel pulsed magnetron sputter technique utilizing very high target power densities. Surface and Coatings Technology. 1999, Vol.122, No.2-3, pp 290–293, ISSN 02578972

[Mattox 2010] Mattox, D. M. Handbook of physical vapor deposition (PVD) Processing. 2nd ed. Amsterdam: Elsevier, 2010. ISBN 978-0-81-552037-5

[Bradley 2001] Bradley, J. W., Thompson, S. and Gonzalvo, Y. A. Measurement of the plasma potential in a magnetron discharge and the prediction of the electron drift speeds. Plasma Sources Science and Technology, 2001, Vol.10, No.3, pp 490–501, ISSN 0963-0252

[Christou 2000] Christou, C., Barber, Z. H. Ionization of sputtered material in a planar magnetron discharge. Journal of Vacuum Science & Technology, 2000, Vol.18, No.6., pp 2897– 2907

[Gudmundsson 2012] Gudmundsson, J. T. High power impulse magnetron sputtering discharge. Journal of Vacuum Science & Technology, 2012, Vol.30, No.3, ISSN 0734-2101

[Bohlmark 2005] Bohlmark, J., Alami, J., Christou, C., Ehiasarian, A. P. and Helmersson, U. Ionization of sputtered metals in high power pulsed magnetron sputtering. Journal of Vacuum Science & Technology, 2005, Vol.23, No.1, pp 18–22, ISSN 0734-2101

[Alami 2005] Alami, J., Persson, P. O. Å., Music, D., Gudmundsson, J. T., Bohlmark, J., Helmersson, U. Ion-assisted physical vapor deposition for enhanced film properties on nonflat surfaces. Journal of Vacuum Science & Technology, 2005, Vol.23, No.2, pp 278–280, ISSN 0734-2101

[Sarakinos 2007] Sarakinos, K., Alami, J., Wuttig, M. Process characteristics and film properties upon growth of TiO x films by high power pulsed magnetron sputtering. Journal of Physics D: Applied Physics, 2007, Vol.40, No.7, pp 2108–2114, ISSN 0022-372

[Schultrich 1988] Schultrich, B., Poessnecker, I. Thermal conductivity of cemented carbides. Journal of Thermal Analysis, 1988, Vol. 33, pp 305 –310.

CONTACTS:

prof. Ing. Miroslav Piska, CSc., Bc. Tereza Havlikova
Brno University of Technology, Faculty of Mechanical Engineering
Department of Manufacturing Technology
Technicka 2896/2, Brno, 616 69, Czech Republic
tel. : +420 541 142 5555
e-mail : piska@fme.vutbr.cz

[Engwall 2019] Engwall, A. M., Shin, S. J., Bae, J., Wang, Y. M. Enhanced properties of tungsten films by high-power impulse magnetron sputtering. Surface and Coatings Technology, 2019, Vol.363, pp 191–197, ISSN 02578972

[Samuelsson 2010] Samuelsson, M., Lundin, D., Jensen, J., Raadu, M. A., Gudmundsson, J. T., Helmersson, U. On the film density using high power impulse magnetron sputtering. Surface and Coatings Technology, 2010, Vol.205, No.2, pp 591–596

[Ehiasarian 2007] Ehiasarian, A.P., Wen, J. G., Petrov, I. Interface microstructure engineering by high power impulse magnetron sputtering for the enhancement of adhesion. Journal of Applied Physics, 2007, Vol.101, No.5, ISSN 0021-8979

[Alami 2007] Alami, J., Eklund, P., Andersson, J. M., Lattemann, M., Wallin, E., Bohlmark, J., Persson, P., Helmersson, U. Phase tailoring of Ta thin films by highly ionized pulsed magnetron sputtering. Thin Solid Films, 2007, Vol.515, No.7–8, pp 3434–3438, ISSN 00406090

[Greczynski 2014] Greczynski, G., Lu, J., Jensen, J., Bolz, S., Kolker, W., Schiffers, Ch., Lemmer, O., Greene, J. E., Hultman, L. A review of metal-ion-flux-controlled growth of metastable TiAlN by HIPIMS/DCMS co-sputtering. Surface and Coatings Technology, 2014, Vol.257, pp 15–25, ISSN 02578972

[Bohlmark 2006] Bohlmark, J., Östbye, M., Lattemann, M., Ljungcrantz, H., Rossell, T., Helmersson, U. Guiding the deposition flux in an ionized magnetron discharge. Thin Solid Films, 2006, Vol.515, No.4, pp 1928–1931, ISSN 00406090

[CemeCon s.r.o. 2022] CemeCon, FerroCon (HiPIMS). CemeCon s.r.o., 2022, Ivancice [online], October 3rd 2022, Available from https://www.cemecon.cz/povlakovani-ferrocon-hipims

[Kalss 2006] Kalss, W., Reiter A., Derflinger V., Gey, C. Endrino J.L. Modern coatings in high performance cutting applications. International Journal of Refractory Metals & Hard Materials, 2006, Vol.24, pp 399–404.